Protection Elements for Self-Healing Microgrids Using Only Local Measurements

Elijah Silva¹, Olga Lavrova¹

¹ Electrical and Computer Engineering Department, Klipsch School of Electrical and Computer Engineering New Mexico State University, Las Cruces, NM 88003 Eli01@nmsu.edu

Abstract— There are unique challenges associated with protection and self-healing of microgrids energized by multiple inverter-based distributed energy resources. In this study, prioritized undervoltage load shedding and undervoltage-supervised overcurrent (UVOC) for fault isolation are demonstrated using PSCAD. The PSCAD implementations of these relays are described in detail, and their operation in a self-healing microgrid is demonstrated.

Index Terms—PSCAD, load-shedding, protections, fault, Grid forming inverter, inverter based resource.

I. Introduction

Microgrids energized by inverter-based distributed energy resources (IBDERs) could play a significant role in improving power system resilience to major events [1]. Significant challenges exist in the protection and self-healing of such systems [1-5]. These challenges can in general be addressed using communications-based protection and control [6,7], but the cost, reliability, scalability, cybersecurity, and complexity of communications-based systems put them out of reach of many potential microgrid users [8]. Thus, systems relying only on local measurements are important, either for use on their own in highly cost-constrained applications or as a backup to a communications-based system. The family of undervoltagebased tools, such as undervoltage load shedding and undervoltage-based protection, is often suggested for use in systems using only local measurements, but undervoltagebased tools have well-known shortcomings, including that they can be effective at detecting the existence of faults and overloads, but not their locations [9].

This work focuses on the study of undervoltage-based systems for local-measurement-based protection, self-healing and self-networking of IBDER-based microgrids for resilience. The protection system concept, in [10], includes:

- Load relays, which connect individual loads to the system.
 The load relays include undervoltage load shedding, underfrequency load shedding, and overcurrent functions.
- Line relays, which separate the system into sections or zones. The line relays include undervoltage, overcurrent, and synchronization check functions, among others.

In this paper, a candidate load relay design is described in detail. A PSCAD model of the load relay is presented, and the load relay is demonstrated using PSCAD models of the IEEE 13-bus distribution test feeder [11]. The use of undervoltage-

Michael Ropp²

Sandia National Laboratories,
Albuquerque, NM, 87185

meropp@sandia.gov

supervised overcurrent (UVOC) for fault isolation is described.

II. CONCEPTS AND SIMULATION MODELS

A. Load prioritization

Load shedding is routinely used to maintain generation-load balance in a power system. In systems energized by rotating machines, a decrease in frequency is used to indicate an overload, and underfrequency load shedding can be utilized to restore generation-load balance. In systems energized by IBDERs, the frequency may decline with loading if the IBDERs have frequency droop controls, but when the inverters become overloaded they will reach their current limits, at which point they cease regulating voltage and produce their maximum current (or they trip offline, in which case the system will likely collapse). Thus, faults and overloads will lead to a systemwide undervoltage, and undervoltage load shedding can be used in place of underfrequency load shedding. The least critical loads are shed first, with more critical loads only being shed if the undervoltage persists. A time-undervoltage function is used, as shown in Fig. 1.

In this work, loads are classified into Groups A, B and C, with A being the most critical and C being the least critical. When an undervoltage occurs, Group C will be shed first. If after some time the load relays still detect undervoltage, the system will shed the Group B loads according to the Group B time-undervoltage curve. Group A will always be shed last, if at all. Load energization follows the opposite priority logic: as soon as the voltage is within the nominal range for a prescribed time, Group A will be energized, then Group B, and finally Group C. The trip time for each load Group at each undervoltage level is shown in Fig. 1.

B. Load relay implementation in PSCAD

The load relays demonstrated here include under/overvoltage, overcurrent, and under/overfrequency functions. Values that fall outside the accepted ranges will result in a trip signal from any of the load relay functions. Each load will have a load relay associated with it, and each load relay has its own meter reading voltage and current (the frequency is derived from the voltage).

The PSCAD implementation of the load relays includes a delayed-enable function, shown in Fig. 2, that feeds the relay functions nominal values until after a user-set time has elapsed. This is to prevent the load relays from misbehaving during initialization of the system.

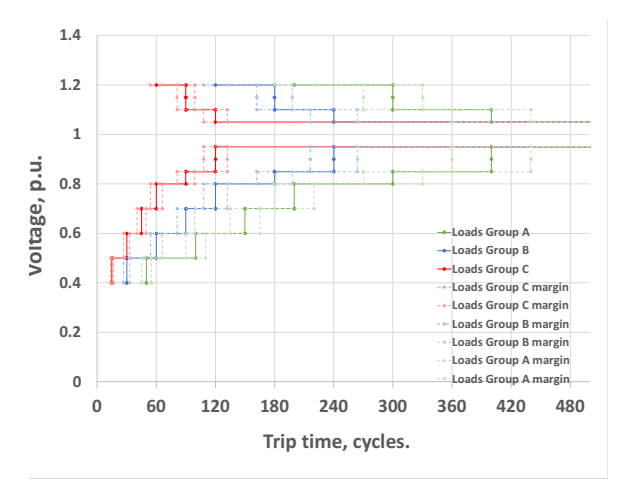


Figure 1 Load group trip times

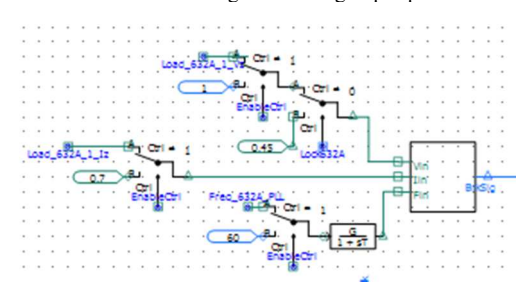


Figure 2 Load relay top-level design

C. Undervoltage Trip logic

In the implementation presented here, the Group A, B and C undervoltage trip levels are the same for all Groups, and differentiation is achieved using the timing. The undervoltage levels used here are:

- Case 1: $1.0*10^{-1} < V < 0.7$
- Case 2: 0.7001 < V < 0.8
- Case 3: 0.8001 < V < 0.9
- Case 4: 0.9001 < V < 0.95
- Case 5: V > 1.1

Undervoltage logic consists of two comparators connected to a NOR gate, as shown in Fig. 3. The two comparators set the upper lower bounds. If the voltage lies between the thresholds, downstream logic then determines which time delay to apply.

D. Frequency Trip logic

The frequency logic in the load relays is shown in Fig. 4. The frequency of the voltage is measured by a phase-locked loop (PLL), and the PLL-measured frequency is then filtered using a low-pass filter.

E. Overcurrent Trip logic

The load relays also include an instantaneous overcurrent function with a user-settable trip threshold. The logic for the instantaneous overcurrent is shown in Fig. 5.

F. Voltage reclosure logic

After the voltage has returned to within the nominal band for a selected length of time, the load relay may reclose. The voltage reclosure logic (Fig. 7) is similar to the undervoltage load shedding logic, except that in this case there is only one voltage range.

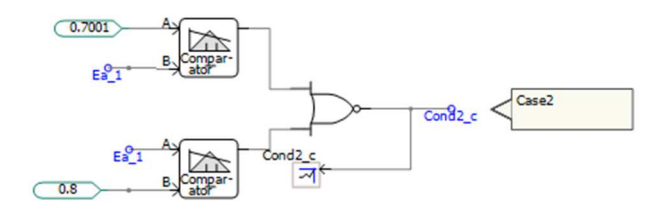


Figure 3 Undervoltage case comparator circuit

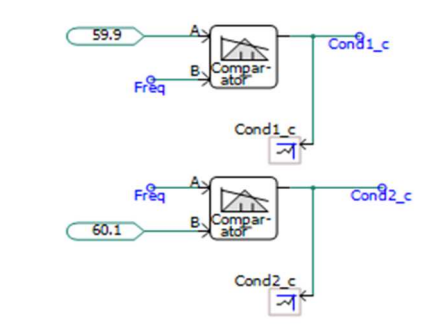


Figure 5. Frequency Trip logic

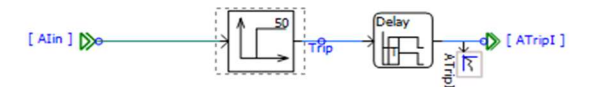


Figure 6. Current Trip logic

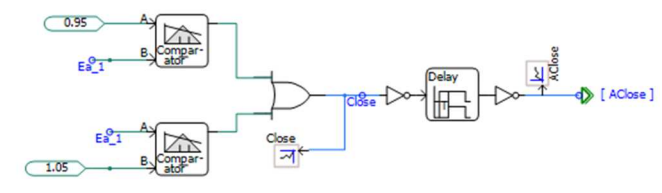


Figure 7 Undervoltage closing logic

G. Frequency reclosure logic

The frequency reclosure logic (Fig. 8) is simply the inverse of the frequency tripping logic since both have the same range.

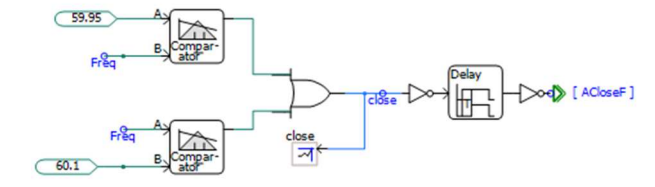


Figure 8 Frequency closing logic

H. Undervoltage-supervised overcurrent

The undervoltage elements do not allow determination of the location of a fault by themselves. If a fault is persistent, then during self-reassembly of the system one of the line or load relays will reclose onto the fault. Reclosure onto a fault is detected using undervoltage-supervised overcurrent (UVOC). If a relay sees nominal voltage and recloses onto a fault, the voltage will immediately drop again and that relay will detect high current. If this combination of undervoltage and overcurrent occurs within a short time after reclosure, the UVOC function will assume that the relay has reclosed onto a fault and will re-open the breaker. The UVOC implementation in PSCAD is shown in Fig. 9. The time delimitation of the UVOC signal is achieved using a read signal that lasts for one-third of a second after breaker closure, and is AND-ed with the undervoltage and overcurrent functions, as shown in Fig. 6. If all three criteria (voltage low, current high, and within the time period after breaker reclosure) are met simultaneously, the UVOC function asserts and re-opens the breaker.

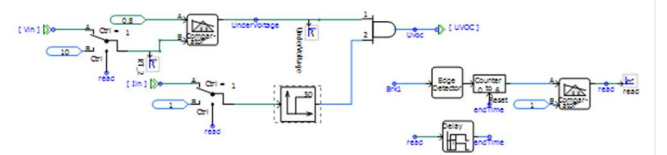


Figure 9. UVOC detection circuit

I. Random delay element

It is generally desirable that no two load or line relays operate at exactly the same time. To help to achieve this, a random element is added to the reclosure time of each line and load relay. Even with this provision, there is a finite probability that two adjacent relays could generate the same random number, and this probability must be minimized. The probability of two relays generating the same random delay value can be calculated using traditional discrete probability theory. The discrete sample space for random delays for relays in Groups B and C are shown in Table 1. It is assumed that random delays between 0 and 9 seconds will be considered, where each delay can be an integer value or decimal value.

TABLE 1. SAMPLE SPACE FOR RANDOM DELAY CLOSING.

Relay Group	Delay value	Sample space with integer delay	Sample space with decimal delay
Group A	0	{0}	{0}
Group B	5sec+random delay, between 0 and 9	{5, 6 14}	{5, 5.1, 5.2, 5.313.8, 13.9,14}
Group C	15sec+random delay, between 0 and 9	{15, 16, 24}	{15, 15.1, 15.2, 23.8, 23.9,14}

If the increment between random numbers is 1 s, then the probability of two out of three relays closing at the same time is:

Probability of two out of three relays closing at the same time is:
$$P_{k \text{ out of } n \text{ relays}} = \frac{C_2^3 \cdot n \cdot (n-1)}{10^n} = \frac{3 \cdot 10 \cdot 9}{10^3} = 0.27 \text{ (4)}$$

where C_k^n is a binomial distribution coefficient ("n choose k"). If the increment between random delays is 0.1 s instead of 1 s, then the probability of two out of any three relays simultaneously reclosing becomes

$$P_{k \text{ out of } n \text{ relays}} = \frac{C_2^3 \cdot 100 \cdot (100 - 1)}{100^n} = 0.0297 \quad (5)$$

The probability of two out of four relays closing at the same time can be found as:

$$P_{k \ out \ of \ n \ relays} = \frac{C_2^4 \cdot 10 \cdot (10 - 1)}{10^n} = 0.54 \tag{6}$$

If the delay is quantized in decimal seconds, then probability can be found as.

$$P_{k \text{ out of } n \text{ relays}} = \frac{C_2^3 \cdot 100 \cdot (100 - 1)}{100^n} = 0.0594$$
 (7)

And lastly, probabilities for three out of four for integer

$$P_{k \ out \ of \ n \ relays} = \frac{C_3^4 \cdot 10 \cdot (10 - 1)}{10^n} = 0.36 \tag{8}$$

and for decimals

$$P_{k \text{ out of } n \text{ relays}} = \frac{C_2^3 \cdot 100 \cdot (100 - 1)}{100^n} = 0.0396$$
 (9)

TABLE 2. PROBABILITIES OF LINE AND LOAD RELAYS CLOSING.

	Delay value: integer sec	Delay value: decimal sec
Two line relays closing	10%	1%
Two out of three load relays	27%	2.97%
Three out of four load relays	36%	3.96%
Two out of four load relays	54%	5.94%

This result demonstrates the importance of selecting the smallest practical increment for the random delay element in the reclose timing. Given the speed with which relays operate, it seems unlikely that quantization with smaller increments than 0.1 s would be feasible.

III. RESULTS

These protection elements were demonstrated in PSCAD in the IEEE 13-bus distribution test circuit [11]. For this work, the 13-bus feeder was divided into three microgrids, each with its own IBDER, as shown in Fig. 10. In Fig. 10, the dashed lines across the figure indicate the microgrid boundaries, and the heavy black squares toward the right show the locations of the three IBDERs. The microgrids can be interconnected via Microgrid Boundary Relays (MBRs), which are labeled in red in Fig. 10.

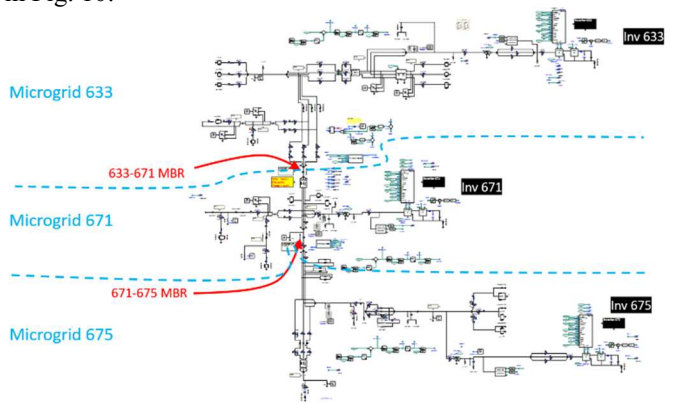


Figure 10. IEEE- 13 Bus feeder

A. Test Case I

Test Case I included two sequential 1LG faults on bus 632 of the 13-bus system. The first fault occurred at 22 seconds and lasted for 2 seconds, and the second was at 35 seconds and lasted for 5 seconds. The simulation was run twice to verify that the random element was changing as desired. Tables 3-7 summarize the results. These results indicate that load groups are tripping in the correct order as expected, the random timing element is varying as expected, and the loads self-restore in the expected order.

TABLE 3. TRIPPING TIMES FOR LOAD 632 (FIRST SIM)

Tripping Times with Faults	22	35
at 22 and 35 sec (first sim)		
A	23.535	36.518
В	23.098	53.931
С	22.501	35.4725

TABLE 4. TRIPPING TIMES FOR LOAD 632 (SECOND SIM)

Tripping Times with Faults at 22 and 35 sec (second sim)	22	35
A	23.619	36.510
В	22.975	35.933
С	22.493	35.471

TABLE 5. TRIPPING TIMES FOR LOAD 632 (FIRST SIM)

Tripping Times with Faults at 22 and 35 sec (first sim)	22	35
A	23.535	36.518
В	23.098	53.931
С	22.501	35.4725

TABLE 6. CLOSING TIMES FOR LOAD 632 (FIRST SIM)

Closing Times with Faults at	22	35
22 and 35 sec (first sim)	26.734	41 902
A		41.803
В	27.301	42.354
C	27.8	43.034

TABLE 7. CLOSING TIMES FOR LOAD 632 (SECOND SIM)

TIBLE // CECSHIO THILESTONE	311B 0E = (31	300112 51111)
Closing Times with Faults at	22	35
22 and 35 sec (second sim)		
A	26.685	41.795
В	27.153	42.271
С	27.773	42.905

B. Test Case II

Test Case II was implemented to demonstrate UVOC. The load Group assignments are shown in Table 8.

TABLE 8. LOAD GROUP ASSIGNMENTS.

Group A	Group B	Group C
Load 634	Load 632	Load 645
	Load 652	Load 646
	Load 671	Load 611

In this test, Microgrid 633 (at the top of Fig. 10) was isolated from the other two microgrids. A permanent 1LG fault was

applied at t = 15 seconds near Load 611. Figure 11 shows the breaker status of (top) and voltage at (bottom) of relay R_611, which is associated with load 611. (PSCAD's switch logic is such that a 0 signal corresponds to a closed relay and 1 corresponds to an open relay.)

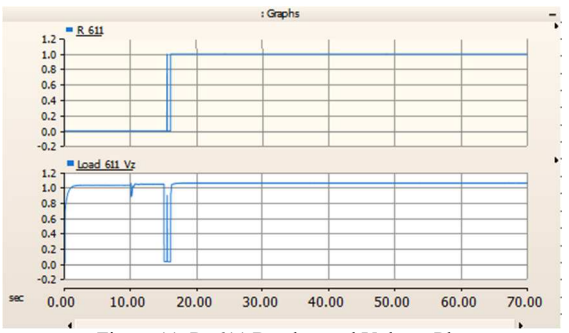


Figure 11. R 611 Breaker and Voltage Plot

After the fault occurs at $t=15\,$ s, $R_611\,$ opens on undervoltage. The voltage returns to within the normal band. $R_611\,$ recloses, but immediately thereafter the voltage collapses and the current rises sharply, triggering the UVOC function. UVOC re-opens R_611 , isolating the fault. The rest of the system then proceeds to restore itself

IV. CONCLUSIONS

This paper presents demonstrations of undervoltage load-shedding relays, self-restoration of the loads using local measurements only, and location and isolation of a fault using undervoltage-supervised overcurrent. PSCAD implementations of all of the protection elements are presented. These concepts and PSCAD models can be effective tools in designing protection of self-healing microgrids energized by IBDERs.

V. ACKNOWLEDGEMENT

This work was partially supported by the NSF Grants \#OIA-1757207 (NM EPSCoR), HRD-1345232, HRD-1914635 and funding from Sandia National Laboratories Campus Executive (CE) LDRD Supplemental Project 20-0656, and award number GR0006770 (SHAZAM), DOE NNSA MSIPP STEP2NLs: DOE Financial Assistance Award # DE-NA0003983 and funding from the Electric Utility Management Program (EUMP) at the New Mexico State University. Sandia National Laboratories is a multi-mission laboratory managed and operated by National Technology and Engineering Solutions of Sandia, LLC., a wholly owned subsidiary of Honeywell International, Inc., for the U.S. Department of Energy's National Nuclear Security Administration under contract DE-NA0003525. The views expressed in the article do not necessarily represent the views of the U.S. Department of Energy or the United States Government. This paper's Sandia ID number is SAND2022-9952 C.

VI. REFERENCES

- R. Campos, C. Figueroa, H. Oyarzun, J. Baeza, "Self-Healing of Electric Distribution Networks: A Review", 7th IEEE International Conference on Computers Communications and Control (ICCCC), May 2018.
- [2]. Li, Z. Chen, L. Fan, P. Zhang, "Toward A Self-Healing Protection and

- Control System", 40th North American Power Symposium, Sept 2008.
- [3]. Y. Liu, R. Fan, V. Terzija, "Power System Restoration: A Literature Review From 2006 to 2016", Journal of Modern Power Systems and Clean Energy 4(3), July 2016, p. 332-341.
- [4]. M. Elgenedy, A. Massoud; S. Ahmed, "Smart grid self-healing: Functions, applications, and developments", First IEEE Workshop on Smart Grid and Renewable Energy (SGRE), March 2015.
- [5]. S. Refaat, A. Mohamed, P. Kakosimos, "Self-Healing Control Strategy: Challenges and Opportunities for Distribution Systems in Smart Grid", 12th IEEE International Conference on Compatibility, Power electronics and Power Engineering, April 2018.
- [6]. D. Lagos, V. Papaspiliotopoulos, G. Korres, N. Natziargyriou, "Microgrid Proection Against Internal Faults", IEEE Power and Energy Magazine May/June 2021, p. 20-35.
- [7]. J. Shiles; E. Wong, S. Rao; C. Sanden; M. A. Zamani; M. Davari; F. Katiraei, "Microgrid protection: An overview of protection strategies in North American microgrid projects", IEEE Power and Energy Society General Meeting 2017, 5 pgs.
- [8]. L. Maurer, A. Stevens, W. Reder, "Tales From the Frontline: Keys to Successful Self-Healing Distribution Projects", IEEE Power and Energy Magazine 10(2), March/April 2012, p. 100-106.
- [9]. M.J. Reno; S. Brahma; A. Bidram; M.E. Ropp, "Influence of Inverter-Based Resources on Microgrid Protection: Part 1: Microgrids in Radial Distribution Systems", *IEEE Power and Energy Magazine* 19(3), April 2021, p. 36-46.
- [10]. M.E. Ropp, O. Lavrova, S. Ranade, A. Ramoko, C. Valdez, "Results of Late-Start LDRD Project 'SHAZAM"". Sandia National Laboratories Report SAND2021-11593, September 2021, Web. doi:10.2172/1821319.
- [11]. IEEE PES Distribution System Analysis Subcommittee Report "Radial Distribution Test Feeders", available online at http://cmte.ieee.org/pestestfeeders/wp-content/uploads/sites/167/2017/08/testfeeders.pdf.

